BJR https://doi.org/10.1259/bjr.20210959

Received: 17 August 2021 | Revised: 11 January 2022 | Accepted: 12 January 2022

Cite this article as:
Busch JJ. The role for MRI-guided transurethral ultrasound ablation in the continuum of prostate cancer care. *Br J Radiol* (2022) 10.1259/bjr.20210959.

INNOVATIONS IN PROSTATE CANCER SPECIAL FEATURE: COMMENTARY

The role for MRI-guided transurethral ultrasound ablation in the continuum of prostate cancer care

JOSEPH J. BUSCH JR., MD

Busch Center, Brookside Concourse 100, Alpharetta, United States

Address correspondence to: Dr. Joseph J. Busch
E-mail: *jbusch@buschcenter.com*

ABSTRACT:

Prostate cancer continues to have a negative impact on the duration and quality of life for males and their families. MRI is transforming the pathway of prostate cancer detection, diagnosis, staging, and surveillance, backed by multiple Level 1 studies and robust reporting standards. This evolving paradigm of MRI-directed care is now being expanded to include in-bore MRI-guided prostate tissue ablation techniques, which reduce the burden of genitourinary complications associated with standard-of-care treatments, without sacrificing cancer control. The workflow for MRI-guided transurethral ultrasound ablation relies on intraprocedural MRI guidance for treatment planning, automated and physician-monitored treatment delivery, and post-treatment assessment at both immediate and long-term time points. Our early experience has identified several procedure refinements, and aligns with early evidence from prospective clinical studies using transurethral ultrasound ablation for treatment of patients with either primary or recurrent disease. Driven by quantitative real-time imaging, MRI-guided ablative interventions provide rich datasets for developing technical refinements and predictive models that will progressively improve patient outcomes as these novel techniques become part of a new standard-of-care.

INTRODUCTION

The continuum of prostate cancer care is being transformed by MRI (Figure 1). Biparametric prostate MRI and MRI-targeted biopsy increase the diagnostic yield for clinically significant cancer while reducing overdiagnosis and overtreatment of clinically indolent disease.[1] Prostate and whole-body MRI can rule out local and distant progression,[2] and multiparametric MRI has an established role in assessing local recurrence and eligibility for local salvage.[3]

The evolving paradigm of MRI-directed prostate cancer care is expanding to include MRI-guided ablation, with the goal of leveraging intraprocedural MRI to directly target, monitor, and control treatment for favourable safety and comparable efficacy to the standard of care. Radical prostatectomy and radiation therapy continue to report high rates of long-term erectile dysfunction, affecting over half of patients after surgery and around a quarter of patients after radiation.[4,5] 2 years after prostatectomy, approximately 20% of men wear pads for urinary incontinence, while around 5% experience rectal toxicity after radiotherapy.[5,6] It is estimated that 10–15% of men with clinically significant disease experience local recurrence or progression after surgery or radiation.[5,6] In light of these shortcomings, patients demand customized therapy that targets and controls cancer while sparing important structures for decreased impact on urinary and sexual function. Here, we describe how MRI-guided transurethral ultrasound ablation (TULSA) exploits the diagnostic and real-time quantitative capabilities of MRI for conformal ablation of prostate tissue, as well as our initial experience with and refinements to the technique.

INTRAPROCEDURAL MRI FOR TREATMENT PLANNING, MONITORING, CONTROL, AND CONFIRMATION

TULSA utilizes intraprocedural MR at each step of its in-bore workflow. The location of the transurethral ultrasound applicator and an endorectal cooling device are registered and adjusted based on 3D T_2 weighted images. Intended ablation contours are then prescribed on axial T_2 weighted images aligned with the 10 independent high-intensity ultrasound elements of the applicator. Together, the directional beams of the linear array of 10 elements are

Figure 1. MRI at the center of prostate cancer care. (A) Biparametric MRI for detection and sequential evaluation of suspicious lesions, used in combination with PSA, DRE, history, and genomics to select candidates for biopsy. The addition of whole-body MRI offers definitive disease staging for patients with high-risk disease. (B) In-bore MRI-targeted biopsy with direct needle and lesion visualization enables accurate tumor sampling. (C) MRI-guided ablation takes advantage of diagnostic-quality intraprocedural T2 and diffusion-weighted images to target prostate cancer lesions with oncological margins and avoid critical structures, while MRI thermometry allows for real-time temperature monitoring and automated feedback control. (D) MRI-based monitoring allows visualization of the acute post-ablation perfusion defect and is used in combination with PSA for surveillance of disease recurrence; the example illustrates immediate and 9 month MRI from a patient treated at our center. DRE, digital rectal examination; PSA, prostate-specific antigen.

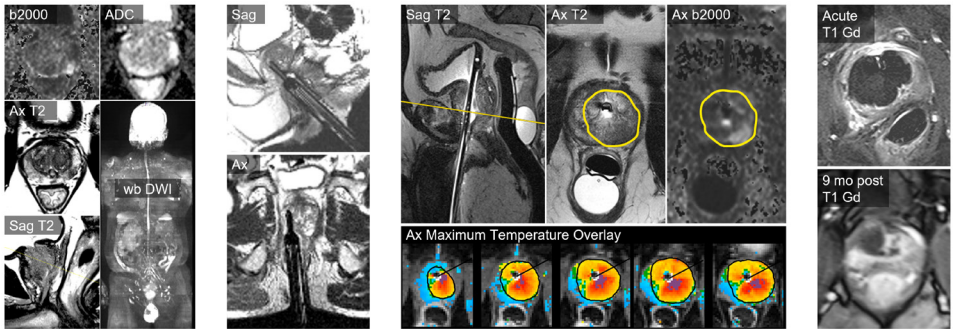

capable of thermally coagulating prostate tissue in a 5 by 0.5 cm blade with a depth of 3 cm from the center of the device. By slowly rotating the applicator, this heating pattern sweeps around through the gland for uniform ablation without cold spots. The urethra and rectum are protected by water cooling.

During treatment, MR images are acquired and used to calculate temperature in real-time, providing continuous volumetric visualization of heating in the prostate and surrounding tissues. MR thermometry exploits the linear relationship between temperature and phase in water-based tissue to calculate temperature difference maps from a series of phase subtraction images acquired continuously during treatment. From temperature images, cumulative temperature and thermal dose maps predictive of treatment effect are calculated and displayed. Unique to TULSA, measured temperatures are also used as quantitative input to a feedback control algorithm that dynamically adjusts the ultrasound intensity and frequency of each treatment element, and the device rotation rate, to ensure that the physician-defined target volume reaches coagulative temperatures of at least 55°C. Temperature maps must be monitored for image artifacts manifested as anomalous temperature measurements in unheated regions to detect gross patient motion, excessive swelling of the gland, contraction of the pelvic floor muscles, displacement of gas in the rectum, or RF interference.

Finally, TULSA incorporates post-treatment contrast-enhanced imaging to directly visualize the thermally-induced hyperacute perfusion defect. While delayed cell kill expands the non-perfused volume in the weeks post-ablation, this image has prognostic value for confirming ablation coverage and the absence of off-target damage.[7] After TULSA, patients are monitored for recurrence with MRI (Figure 1), which mitigates the limitations of PSA testing alone in the post-ablation setting, can better identify patients who need biopsy, and improves the diagnostic accuracy of biopsy when deemed necessary.

INITIAL EXPERIENCE AND FUTURE DIRECTIONS

In our initial experience incorporating MRI-guided ablation with TULSA into a dedicated prostate diagnosis and biopsy practice, we have identified a range of relevant ablation plans and disease settings, some of which have been made possible by several procedure refinements that we have developed.

At our outpatient imaging center, we have made several practical changes that contribute to improvements in treatment efficiency and consistency. First, while other sites perform TULSA under general anesthesia with intubation, at our imaging center we perform monitored anesthesia care with titrated propofol infusion and multimodal pain management, which appears to be better tolerated by patients and has not resulted in significant interruptions due to patient motion as might be expected. Second, we have found that in all but a few patients with known anatomic variations, the applicator can be inserted safely without use of a guidewire which saves time and reduces cost. Third, patients are sent home with an indwelling Foley catheter rather than placing a suprapubic catheter before starting the procedure. While the manufacturer's disposables are a significant part of the procedure cost, the simplifications described above decrease costs for medications and supplies, and the considerable costs associated with time (MRI and personnel: physician, anesthesia, nursing, and technologist). Combined with careful patient selection, device positioning, treatment planning, and having a consistent treatment team, typical TULSA procedure times average about 3 h (Figure 2).

Another refinement we have made at our center is the incorporation of additional imaging sequences for treatment planning.

Figure 2. Average TULSA procedure timing across ten typical cases performed at our imaging center. Patient preparation includes initiation of monitored anesthesia care, insertion of the ultrasound applicator and endorectal cooling device, and positioning the patient in the MRI scanner. Initial survey images are acquired and used to verify optimal device positioning with a clear acoustic path between the ultrasound applicator and the endorectal cooling device. During treatment planning, 3D T_2 weighted images are used for device alignment and fine adjustment, with axial T_2 weighted, high b-value diffusion-weighted imaging, and ADC maps used to prescribe the intended ablation contours. Pausing treatment allows adjustment of target boundaries to account for intraprocedural changes in the prostate or periprostatic structures. Gadolinium-enhanced T_1 weighted images are acquired and reviewed to assess the extent of acute thermal effects before removing devices and recovering the patient. ADC, apparent diffusion coefficient; TULSA, transurethral ultrasound ablation.

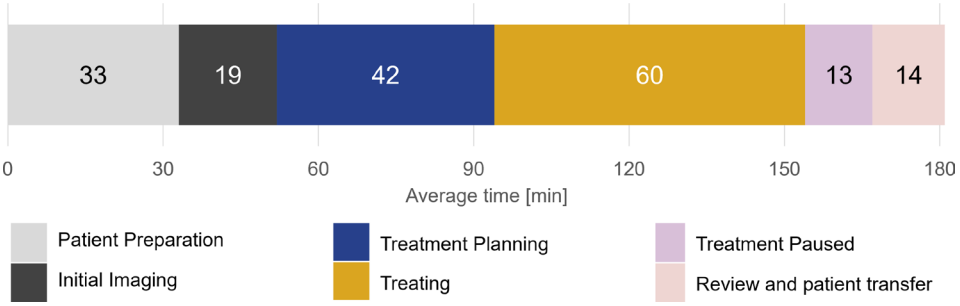

During TULSA, we supplement axial T_2 weighted imaging with intraprocedural calculated b = 2000 s/mm2 diffusion-weighted images and quantitative apparent diffusion coefficient maps aligned with the transducer elements. Combining axial biparametric MRI with sagittal and coronal views of the 3D T_2 weighted planning acquisition enables precise targeting of small lesions, preservation of the neurovascular bundles and ejaculatory ducts, and definition of treatment margins near lesions at the extreme apex (Figure 3). We also employ susceptibility-weighted imaging of intraprostatic calcifications for both patient screening and intraprocedural adjustments of applicator positioning.

With these improvements, we have been able to deliver ablations ranging from small angular sectors targeting individual lesions, up to whole-gland ablation in large prostates requiring two-part ablations within the same session (Figure 4). These personalized treatment plans facilitate shared decision-making with the patient and his family. In our experience, subtotal ablations that treat the whole gland but spare a few millimeters of prostate tissue near the neurovascular bundle contralateral to an index lesion offer an attractive intersection of the oncological advantages of radical treatments with a similar side-effect profile to focal therapy. In TULSA cohorts that allowed sparing of the ejaculatory ducts and neurovascular bundles, antegrade ejaculation has been preserved in approximately 80% of patients,[8,9] compared to 20–30% after whole-gland ablation.[10] Further, the combination of diffusion-weighted imaging to identify disease extent, with control over the frequency of sonication to limit ablation depth, has enabled us to ablate lesions at the extreme apex with minimal heating of the external sphincter and observe no incidence thus far of long-term incontinence.

Figure 3. Patient with PSA 5.1 ng ml^{-1}, prostate volume 28 cc, PIRADS 5 at right posterolateral midline to base. Gleason Score 4 + 3 on systematic biopsy, 6 of 12 systematic cores positive all at right side-of the gland. (A) Intraprocedural 3D T_2 weighted sagittal image displaying ultrasound applicator and endorectal cooling device. ADC map (B), intraprocedural axial T2 (D), and calculated b2000 (E) used to prescribe ablation volume. MRI maximum temperature map (C) achieved during treatment. Non-enhanced tissued attributed to immediate cell death visible on post-treatment contrast enhanced image (F). ADC, apparent diffusion coefficient; PSA, prostate-specific antigen.

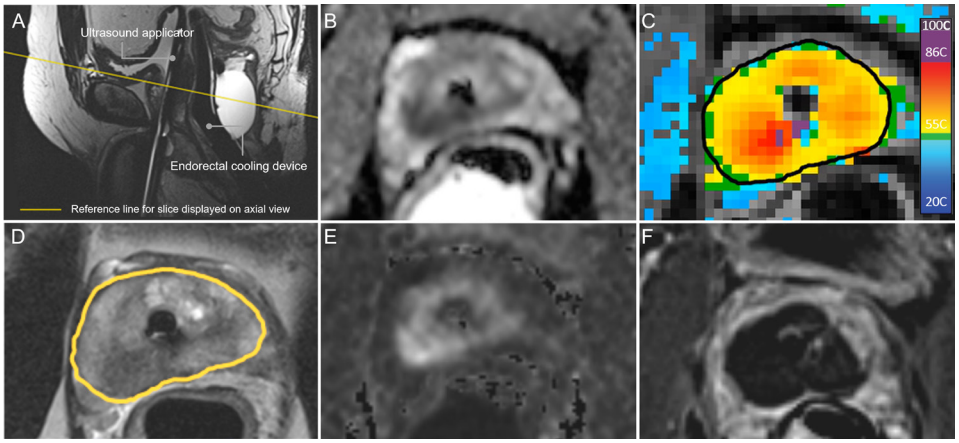

Figure 4. Patient with PSA 3.2 ng ml^{-1}, prostate volume 115 cc, Gleason 4 + 3 diagnosed by TRUS biopsy concordant to PIRADS 4 lesion at extreme apex, with concomitant urinary symptoms associated with benign prostatic hyperplasia. Single-session two-part ablation strategy was for whole-gland treatment including apical cancer and large middle lobe, with tissue sparing at neurovascular bundles and ejaculatory ducts. Intraprocedural 3D T_2 weighted sagittal image displaying ultrasound applicator and endorectal cooling device locations during first (A) and second (D) segments. (B) Targeted ablation of middle lobe axial slice and (E) maximum temperature coverage. Immediate post-TULSA contrast-enhanced images in (C) sagittal and (F) axial views confirm the large ablation volume including the middle lobe. PSA, prostate-specific antigen; TULSA, TULSA, transurethral ultrasound ablation.

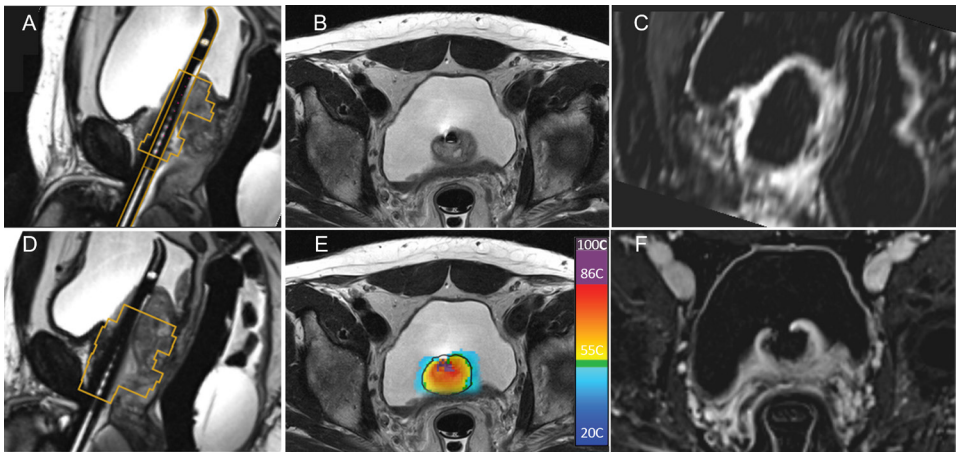

Early trends in PSA kinetics, follow-up multiparametric MRI, and functional outcomes at our center appear to be in line with published studies for TULSA, with no ongoing incontinence, and recatheterization in approximately 5% of patients. In males with localized prostate cancer, the FDA registration study demonstrated that 1 year after a single whole-gland TULSA treatment 79% of patients were free of clinically significant disease, 75% preserved erections sufficient for penetration, and 96% preserved leak-free urinary continence, with 93% free of additional treatment by 2 years.[10] Grade 3 adverse events incurred by 8% of patients included urethral calculus, epididymitis, stricture, urinary tract infection and retention. A single-center clinical service report applying focal through whole-gland TULSA in both primary and recurrent disease reported 88% early oncologic success and 98% preservation of both potency and continence.[8] While not directly comparable because of the broader patient population including multifocal disease, these results are in line with published series on in-bore focal laser ablation[11] and MRI-guided transrectal focused ultrasound.[12] Promising additional applications for TULSA include salvage treatment of radiorecurrent disease, and relief of lower urinary tract symptoms in men with benign prostatic hyperplasia (BPH) concurrent with cancer.[8,13] A small Finnish study of males without cancer seeking BPH treatment reported symptom improvement of 82% with no change in potency.[9] TULSA treatment of prostates as large as 125 cc has been reported,[10] and at our center we have observed urinary symptom improvement in patients treated simultaneously for localized prostate cancer and severe BPH in glands as large as 250 cc (an example with a 115 cc prostate shown in Figure 4). By leveraging MRI to precisely customize ablation for a wide range of tissue volumes, TULSA has the potential to address a variety of prostatic diseases.

Since treatments like TULSA are controlled directly by quantitative imaging data and disposable ultrasound applicators, progressive refinements in treatment algorithms and applicator designs will continue to improve treatment efficacy and safety in the years to come. Also, quantitative analysis of the immense amount of pre-, peri-, and immediate post-operative imaging and clinical data from these procedures yields rich data sets for predictive modeling of patient outcomes that can be refined as the patient progresses through the care continuum. Such technical developments will have a synergistic effect with growing clinician expertise and physician education beyond the manufacturer training, as well as standardization of patient selection, procedure workflow, and protocols for sedation and perioperative care.

CONCLUSION

The integration of MRI across the continuum of prostate cancer care is driving meaningful improvements in disease management for men and their families. The utility of various MR image types in the treatment workflow provides a rationale for expanding the use of in-bore prostate ablation procedures. Our promising early experience with MRI-guided TULSA in treating primary or recurrent cancer and BPH with a range of customized ablation plans aligns with the growing body of evidence suggesting that MRI-guided ablation techniques deliver improved functional preservation over conventional treatments, without compromising cancer control.

REFERENCES

1. Drost F-JH, Osses DF, Nieboer D, Steyerberg EW, Bangma CH, et al. Prostate mri, with or without mri-targeted biopsy, and systematic biopsy for detecting prostate cancer. *Cochrane Database Syst Rev* 2019; **4**: CD012663. https://doi.org/10.1002/14651858.CD012663.pub2
2. Van Nieuwenhove S, Van Damme J, Padhani AR, Vandecaveye V, Tombal B, et al. Whole-body magnetic resonance imaging for prostate cancer assessment: current status and future directions. *J Magn Reson Imaging* 2020. https://doi.org/10.1002/jmri.27485
3. Panebianco V, Villeirs G, Weinreb JC, Turkbey BI, Margolis DJ, et al. (n.d.). Prostate Magnetic Resonance Imaging for Local Recurrence Reporting (PI-RR). In: *International Consensus -based Guidelines on Multiparametric Magnetic Resonance Imaging for Prostate Cancer Recurrence after Radiation Therapy and Radical Prostatectomy. Eur Urol Oncol. 2021 Feb*., pp. 00027–4. https://doi.org/10.1016/j.euo.2021.01.003
4. Hunt AA, Choudhury KR, Nukala V, Nolan MW, Ahmad A, et al. Risk of erectile dysfunction after modern radiotherapy for intact prostate cancer. *Prostate Cancer Prostatic Dis* 2021; **24**: 128–34. https://doi.org/10.1038/s41391-020-0247-x
5. Neal DE, Metcalfe C, Donovan JL, Lane JA, Davis M, et al. Ten-year mortality, disease progression, and treatment-related side effects in men with localised prostate cancer from the protect randomised controlled trial according to treatment received. *Eur Urol* 2020; **77**: S0302-2838(19)30837-1: 320–30: . https://doi.org/10.1016/j.eururo.2019.10.030
6. Nyberg M, Hugosson J, Wiklund P, Sjoberg D, Wilderäng U, et al. Functional and oncologic outcomes between open and robotic radical prostatectomy at 24-month follow-up in the Swedish LAPPRO trial. *Eur Urol Oncol* 2018; **1**: S2588-9311(18)30039-7: 353–60: . https://doi.org/10.1016/j.euo.2018.04.012
7. Mäkelä P, Anttinen M, Suomi V, Steiner A, Saunavaara J, et al. Acute and subacute prostate mri findings after mri-guided transurethral ultrasound ablation of prostate cancer. *Acta Radiol* 2021; **62**: 1687–95. https://doi.org/10.1177/0284185120976931
8. Lumiani A, Samun D, Sroka R, Muschter R. Single center retrospective analysis of fifty-two prostate cancer patients with customized mr-guided transurethral ultrasound ablation (tulsa). *Urol Oncol* 2021; **39**: S1078-1439(21)00173-3: 830. . https://doi.org/10.1016/j.urolonc.2021.04.022
9. Viitala A, Anttinen M, Wright C, Virtanen I, Mäkelä P, et al. Magnetic resonance imaging-guided transurethral ultrasound ablation for benign prostatic hyperplasia: 12-month clinical outcomes of a phase i study. *BJU Int* 2021. https://doi.org/10.1111/bju.15523
10. Klotz L, Pavlovich CP, Chin J, Hatiboglu G, Koch M, et al. Magnetic resonance imaging-guided transurethral ultrasound ablation of prostate cancer. *J Urol* 2021; **205**: 769–79. https://doi.org/10.1097/JU.0000000000001362
11. Walser E, Nance A, Ynalvez L, Yong S, Aoughsten JS, et al. Focal laser ablation of prostate cancer: results in 120 patients with low- to intermediate-risk disease. *J Vasc Interv Radiol* 2019; **30**: S1051-0443(18)31506-9: 401-409. . https://doi.org/10.1016/j.jvir.2018.09.016
12. Ghai S, Finelli A, Corr K, Chan R, Jokhu S, et al. MRI-guided focused ultrasound ablation for localized intermediate-risk prostate cancer: early results of a phase ii trial. *Radiology* 2021; **298**: 695–703. https://doi.org/10.1148/radiol.2021202717
13. Anttinen M, Mäkelä P, Viitala A, Nurminen P, Suomi V, et al. Salvage magnetic resonance imaging-guided transurethral ultrasound ablation for localized radiorecurrent prostate cancer: 12-month functional and oncological results. *Eur Urol Open Sci* 2020; **22**: 79–87. https://doi.org/10.1016/j.euros.2020.10.007